Table 2 Characteristics of HCV RNA-negative or positive patients at week 4, 12, and 24

At week 4	Negative ($n = 18$)	Positive ($n = 132$)	p value
Age (years)	49.5 ± 14.6	57.6 ± 10.3	0.003
HCV RNA (Log IU/mL)	6.0 ± 0.7	6.4 ± 0.7	0.009
At week 12	Negative ($n = 88$)	Positive ($n = 53$)	p value
Core 70 substitution (wild/mutant)	39/14	13/22	<0.001
IL-28B, rs8099917 (TT/non-TT)	31/8	10/18	<0.001
At week 24	Negative ($n = 115$)	Positive ($n = 23$)	p value
Core 70 substitution (wild/mutant)	48/23	4/11	0.003
IL-28B, rs8099917 (TT/non-TT)	38/14	3/10	0.003

Value are mean ± standard deviation (SD)

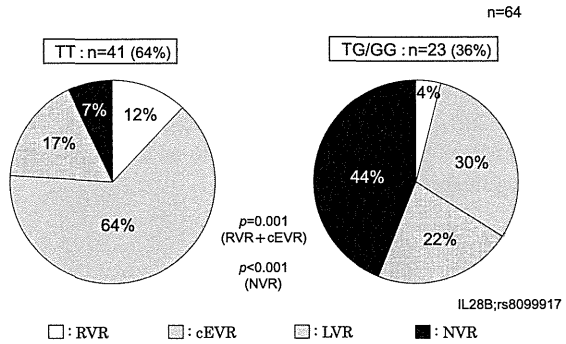

Fig. 4 Treatment response to PEG-IFNα-2a with or without RBV according to the IL-28B single nucleotide polymorphisms (TT versus TG/GG genotype)

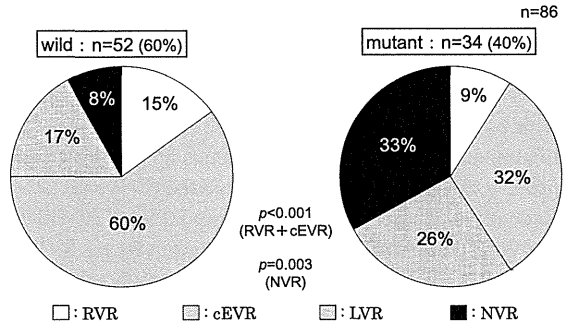

Fig. 5 Treatment response to PEG-IFNα-2a with or without RBV according to the Core 70 mutation (wild-type versus mutant Core 70)

We also investigated the correlation between IL-28B polymorphism and HCV RNA-negative conversion within 12 weeks (RVR + cEVR) in 64 patients in whom IL-28B polymorphism was examined. Negative HCV RNA was achieved within 12 weeks in 76 % of 41 patients with IL-28B TT genotype (major) and in 34 % of 23 patients with IL-28B TG or GG genotype (minor), showing a significant difference between them ($p = 0.001$). Especially in cases with NVR, negative HCV RNA was achieved in 7 % of patients with IL-28B major genotype and in 44 % of patients with IL-28B minor genotype ($p < 0.001$), suggesting that IL-28B polymorphism is strongly associated with treatment response (Fig. 4). Similarly, in 86 patients with determined Core 70 mutation status, negative HCV RNA was achieved within 12 weeks in 75 % of 52 patients with wild-type Core 70 and 41 % of 34 patients with mutant Core 70, showing a significant difference between them ($p < 0.001$). In patients with NVR, the rate of becoming HCV RNA-negative within 12 weeks was 8 % in patients with wild-type Core 70 and 33 % in those with mutant Core 70 ($p = 0.003$) (Fig. 5).

The SVR rates at different time points of HCV RNA-negative conversion by IL-28B polymorphism and Core 70 mutation

The SVR rates were investigated in patients with different time points of HCV RNA-negative conversion (RVR in six patients, cEVR in 33, LVR in 13, and NVR in 13) according to the IL-28B genotypes. The SVR rate was 100 % (5/5) in patients with RVR, 65 % (17/26) in patients with cEVR, 57 % (4/7) in patients with LVR, and 0 % (0/3) in patients with NVR with IL-28B major genotype; whereas the rate was 100 % (1/1) in patients with RVR, 43 % (3/7) in patients with cEVR, 83 % (5/6) in patients with LVR, and 0 % (0/10) in patients with NVR with IL-28B minor genotype. Similarly, the SVR rates were investigated in patients with different time points of HCV RNA-negative conversion (RVR in 11 patients, cEVR in 42, LVR in 18, and NVR in 15) according to the Core 70

Table 3 Characteristics of sustained virological response (SVR) and non-SVR patients

	SVR ($n = 70$)	Non-SVR ($n = 83$)	p value
Age (years)	53.1 ± 12.7	59.4 ± 8.7	<0.001
Gender (male/female)	29/41	34/49	0.954
HCV RNA (Log IU/mL)	6.4 ± 0.7	6.4 ± 0.7	0.782
BMI (kg/m^2)	22.7 ± 3.9	22.9 ± 2.8	0.815
Previous IFN (no/yes)	49/21	44/39	0.032
Fibrosis (F0-2/F3-4)	41/9	31/23	0.007
Activity (A0-1/A2-3)	24/27	25/29	0.938
NS5A mutation, n (0-1/2-)	31/10	47/3	0.013
Core 70 substitution (wild/mutant)	30/11	24/27	0.012
IL-28B, rs8099917 (TT/non-TT)	26/9	17/18	0.027
HCV RNA-negative at week 12 (yes/no)	58/12	30/41	<0.001
Treatment group (B,C,E/A,D,F)	32/38	29/16	0.049

Values are mean ± standard deviation (SD)

BMI body mass index

Table 4 Associated factors with sustained virological response (SVR) by multivariate logistic regression analysis

Factor	Odds ratio	95 % CI	p value
Age (per 1 year)	0.94	0.89–0.98	0.005
Previous IFN (no/yes)	1.62	0.62–4.27	0.323
Fibrosis (F0-2/F3-4)	3.38	1.15–10.8	0.026
NS5A mutation, n (2-/0-1)	7.18	1.32–61.0	0.021
Core 70 substitution (wild/mutant)	2.49	1.51–8.28	0.044
IL-28B, rs8099917 (TT/non-TT)	1.85	0.85-8.61	0.563
HCV RNA-negative at week 12 (yes/no)	7.89	2.92–24.0	<0.001

mutation status. The SVR rate was 100 % (RVR), 58 % (cEVR), 44 % (LVR), and 0 % (NVR) in patients with wild-type Core 70; whereas the rate was 67 % (RVR), 55 % (cEVR), 33 % (LVR), and 0 % (NVR) in patients with mutant Core 70. Thus, when the SVR rates were investigated according to the different time points of HCV RNA-negative conversion, there was no association of IL-28B polymorphism or Core 70 mutation with the SVR rates.

Factors affecting the SVR rate

An univariate analysis in 70 SVR patients and 83 non-SVR patients identified age, previous IFN treatment, fibrosis, NS5A mutation, Core 70 mutation, EVR, IL-28B, and treatment group as factors affecting the SVR rate (Table 3). In this analysis, we examined 83 non-SVR patients: 45 non-SVR patients are presented in Fig. 3, and 38 non-SVR patients (23 patients with NVR and 15 patients who discontinued the Peg-IFN-RBV treatment prior to the enrollment of the randomized trial) are presented in Fig. 2. Multivariate analysis using a logistic regression analysis revealed age (younger), fibrosis (mild), NS5A mutation (two or more mutations), Core 70 status (wild-type), and EVR (RVR + cEVR), to be independent factors affecting the SVR rate, and among them EVR was the most significant factor (odds ratio, 7.89; $p < 0.001$) (Table 4). Therefore, even in patients considered intractable based on the IL-28B genotype or Core 70 mutation status, SVR is expected to be achieved once RVR or cEVR is reached during treatment.

Discussion

The introduction of combined treatment with PEG-IFN and RBV has increased the SVR rate to approximately 40–50 % even in intractable cases with genotype 1b high virus titer chronic hepatitis C after a standard treatment course of 48 weeks [1–4]. In an attempt to further improve the SVR rate, we propose a concept of "response-guided therapy", in which the treatment regimen (such as an extension of a treatment period) is determined according to the viral response to the initial treatment [7–15]. In cases with positive HCV RNA at week 4 or 12, extension of the treatment period from 48 to 72 weeks has been reported to prevent the recurrence and improve the SVR rate [12–14]. Recently, Miyase et al. [34] showed that PEG-IFNα-2a/ribavirin combination therapy resulted in better SVR rates than PEG-IFNα-2b/ribavirin combination therapy in female, older or low-weight patients. In addition, Minami et al. [35] reported that the rate of severe adverse events was not negligible in PEG-IFN/ribavirin combination therapy, and the rate was affected by treatment regimens. Therefore, it is important to establish a treatment regimen of PEG-IFN/RBV combination therapy that has a high efficacy with minimal adverse events. We herein investigated the treatment regimens based on the concept of response-guided therapy to minimize the rate of treatment discontinuation, without changing the treatment period, in consideration of aged patients in Japan.

Factors influencing SVR have been evaluated in many studies that reported IL-28B (a host factor) and Core 70 mutation (a viral factor) as factors predicting the treatment outcome [23, 24, 36–38]. Our present study also demonstrate that the SVR rate was lower in patients with IL-28B minor genotype and those with mutant Core 70, suggesting that IL-28B polymorphism and Core 70 mutation represent factors largely influencing the negative conversion of HCV RNA. Regarding the correlation between treatment response and SVR, Thompson et al. [38] reported that RVR and cEVR rates were lower in patients with the IL-28B minor genotype than in those with the major genotype but the SVR rate was not affected by the IL-28B genotype in patients with RVR or cEVR. In recent studies published after recognition of IL-28B polymorphism, virological response at week 4 and 12 was highly associated with SVR [39, 40]. In our present results, if RVR or EVR is achieved, a high SVR rate can be obtained regardless of the IL-28B polymorphism or Core 70 mutation status.

If RVR is achieved, PEG-IFNα-2a monotherapy exhibits a treatment effect equivalent to that of PEG-IFNα-2a/RBV combination therapy. Conversely, one patient receiving PEG-IFNα-2a/RBV combination therapy developed anemia caused by RBV, resulting in treatment discontinuation and non-SVR. In a phase III clinical trial in Japanese patients, the SVR rate in patients with RVR was 100 % (14/14) in control patients receiving PEG-IFNα-2a monotherapy but was 78 % (18/23) in those receiving PEG-IFNα-2a/RBV combination therapy [41]. Therefore, in terms of preventing treatment discontinuation due to adverse events of RBV, PEG-IFNα-2a monotherapy is recommended in cases with RVR.

In cases with cEVR, the SVR rate in patients who received biweekly PEG-IFNα-2/RBV combination therapy was comparable or even higher as compared to those who received weekly PEG-IFNα-2/RBV combination therapy. This means that biweekly PEG-IFNα-2a in a later treatment period did not reduce the antiviral effects in a subset of cases achieving a good antiviral effect (cEVR). This is partly because the half-life of PEG-IFNα2a is longer than that of PEG-IFNα2b [42–44], thus enabling the maintenance of antiviral effects. Therefore, this biweekly regimen appears possible only with PEG-IFNα2a. Regarding treatment discontinuation, the rate of treatment discontinuation was 3 % (1/31) in patients receiving biweekly PEG-IFNα-2 and 15 % (6/39) in those receiving weekly PEG-IFNα-2, suggesting that the reduced rate of adverse events and subsequent treatment discontinuation by biweekly administration may lead to the increased SVR rate.

Ikeda et al. [19] reported that one of the HMG-CoA reductase inhibitors, FLV, exhibits inhibitory effects on HCV RNA replication in a system of HCV RNA replication clone. In the clinical setting, Sezaki et al. and Rao and Pandya [20–22] reported that combined use of FLV from the treatment initiation period improved the SVR rate [21]. The HCV RNA is replicated using the lipid droplet in hepatocytes [45, 46], and HMG-CoA reductase inhibitors are reported to inhibit the proliferation of HCV RNA by suppressing the synthesis of mevalonic acid through geranylgeranylation [47].

We investigated whether the SVR rate is improved by the addition of FLV only in cases with LVR, because a high SVR rate is expected in patients showing rapid negative conversion of HCV RNA (such as RVR and cEVR cases) without the combined use of FLV. Our results showed that combined use of FLV yielded a higher SVR rate (62 %) as compared to the rate (29 %) obtained without the use of FLV, suggesting that the difference in the recurrence rate may reflect the difference in the SVR rate in patients negative for HCV RNA. Thus, because we used FLV in patients with LVR at high risk of recurrence, but not in those with RVR or cEVR at low risk of recurrence, the difference in anti-HCV activities by FLV was more pronounced. It has been reported that treatment with HMG-CoA reductase inhibitors does not increase the risk of severe hepatotoxicity in patients with chronic hepatitis C [48], which is consistent with our present results showing no adverse events associated with the addition of FLV.

In summary, the SVR rate was 52 % (32/61) in the group receiving PEG-IFNα-2a/RBV combination therapy and 70 % (38/54) in the group receiving modified treatment regimens according to response-guided therapy, showing a significant increase in the latter group. This result may be attributed to the difference in the rate of treatment discontinuation, which was significantly lower in the response-guided therapy group [2 % (1/54)] than in the PEG-IFNα-2a/RBV combination group [11 % (7/61)]. In addition, anti-HCV effects of FLV in patients with LVR at high risk of recurrence may contribute to the improved SVR in the response-guided therapy group. Our results demonstrated the safety and efficacy of PEG-IFNα-2a monotherapy in patients with RVR, biweekly PEG-IFNα-2a/RBV combination therapy in those with cEVR, and PEG-IFNα-2a/RBV/FLV combination therapy in those with LVR.

In conclusion, for the treatment of genotype 1b high virus titer chronic hepatitis C, the selection of an optimal response-guided therapy option, taking into consideration the viral response to initial treatment, the IL-28B polymorphism and Core 70 mutation status, and the safety of individual patients, can improve the SVR rate.

Acknowledgments We thank Ms. R. Nakatani for her assistance with data collection. We also thank Ms. N. Kanazawa for her excellent lab work on IL28B SNPs and Core 70 substitution in this study.

Conflict of interest Shuhei Nishiguchi received financial support from Chugai pharmaceutical, MSD, Dainippon Sumitomo Pharma,

Ajinomoto Pharma, and Otsuka pharmaceutical. The remaining authors declare no conflict of interest.

References

1. Manns MP, McHutchison JG, Gordon SC, et al. Peginterferon alfa-2b plus ribavirin compared with interferon alfa-2b plus ribavirin for initial treatment of chronic hepatitis C: a randomized trial. Lancet. 2001;358:958–65.
2. Fried MW, Shiffman ML, Reddy KR, et al. Peginterferon alfa-2a plus ribavirin for chronic hepatitis C virus infection. N Engl J Med. 2002;347:975–82.
3. Kuboki M, Iino S, Okuno T, Omata M, et al. Peginterferon a-2a (40 KD) plus ribavirin for the treatment of chronic hepatitis C in Japanese patients. J Gastroenterol Hepatol. 2007;22:645–52.
4. Yamada G, Iino S, Okuno T, et al. Virological Response in patients with hepatitis C virus genotype 1b and a high viral load impact of peginterferon-α-2a plus ribavirin dose reductions and host-related factors. Clin Drug Invest. 2008;28(1):9–16.
5. Kumada H, Toyota J, Okanoue T, Chayama K, Tsubouchi H, Hayashi N. Telaprevir with peginterferon and ribavirin for treatment-naive patients chronically infected with HCV of genotype 1 in Japan. J Hepatol. 2012;56:78–84.
6. Hayashi N, Okanoue T, Tsubouchi H, Toyota J, Chayama K, Kumada H. Efficacy and safety of telaprevir, a new protease inhibitor, for difficult-to-treat patients with genotype 1 chronic hepatitis C. J Viral Hepatol. 2012;19:e134–42.
7. Imai Y, Tamura S, Tanaka H, et al. Reduced risk of hepatocellular carcinoma after interferon therapy in aged patients with chronic hepatitis C is limited to sustained virological responders. J Viral Hepatol. 2010;17:185–91.
8. Tanaka T, Shakado S, Morihara D et al. The prognostic factors of sustained virologic response among patients of chronic hepatitis C treated with peg-interferon alpha 2a monotherapy. Kanzo 2008;49:417–25.
9. Berg T, von Wagner M, Nasser S, et al. Extended treatment duration for hepatitis C virus type 1: comparing 48 versus 72 weeks of peginterferon-alfa-2a plus ribavirin. Gastroenterology. 2006;130:1086–97.
10. Sanchez-Tapias JM, Diago M, Escartin P, et al. Peginterferon-alfa2a plus ribavirin for 48 versus 72 weeks in patients with detectable hepatitis C virus RNA at week 4 of treatment. Gastroenterology. 2006;131:451–60.
11. Ferenci P, Laferl H, Scherzer TM, et al. Peginterferon alfa-2a/ribavirin for 48 or 72 weeks in hepatitis C genotypes 1 and 4 patients with slow virologic response. Gastroenterology. 2010; 138:503–12.
12. Pearlman BL, Ehleben C, Saifee S. Treatment extension to 72 weeks of peginterferon and ribavirin in hepatitis c genotype 1-infected slow responders. Hepatology. 2007;46:1688–94.
13. Nabci C Teoh et al. Individualisation of antiviral therapy for chronic hepatitis C. J Gastroenterol Hepatol. 2010; 25:1206–16.
14. Reddy KR, Lin F, Zoulim F. Response-guided and -unguided treatment of chronic hepatitis C. Liver Int. 2012;32:64–73.
15. Di Martino V, et al. Response-guided peg-interferon plus ribavirin treatment duration in chronic hepatitis C: meta-analyses of randomized, controlled trials and implications for the future. Hepatology. 2011;54:789–800.
16. Zeuzem S, et al. Pegylated-interferon plus ribavirin therapy in the treatment of CHC: individualization of treatment duration according to on-treatment virologic response. Curr Med Res Opin. 2010;26:1733–43.
17. Franik H, et al. Meta-analysis shows extended therapy improves response of patients with chronic hepatitis C virus genotype 1 infection. Clin Gastroenterol Hepatol. 2010;8:884–90.
18. Yu ML, Dai CY, Huang JF, et al. Rapid virological response and treatment duration for chronic hepatitis C genotype 1 patients: a randomized trial. Hepatology. 2008;47:1884–93.
19. Ikeda M, Abe K, Yamada M, et al. Different anti HCV profiles of statins and their potential for combination therapy with interferon. Hepatology. 2006;44:117–25.
20. Sezaki H,Suzuki F,Akuta N et al. Influence of HMG-CoA reductase inhibitor to virological response of peginterferon/ribavirin combination therapy in chronic hepatitis C. Kanzo 2008: 49;22–4.
21. Sezaki H, Suzuki F, Akuta N, et al. An open pilot study exploring the efficacy of fluvastatin, pegylated interferon and ribavirin in patients with hepatitis C virus genotype 1b in high viral loads. Intervirology. 2009;52:43–8.
22. Rao GA, Pandya PK. Statin therapy improves sustained virologic response among diabetic patients with chronic hepatitis C. Gastroenterology. 2011;140:144–52.
23. Akuta N, Suzuki F, Kawamura Y, et al. Predictive factors of early and sustained responses to peginterferon plus ribavirin combination therapy in Japanese patients infected with hepatitis C virus genotype 1b: amino acid substitutions in the core region and low-density lipoprotein cholesterol levels. J Hepatol. 2007;46:403–10.
24. Akuta N, Suzuki F, Sezaki H, et al. Association of amino acid substitution pattern in core protein of hepatitis C virus genotype 1b high viral load and non-virological response to interferon-ribavirin combination therapy. Intervirology. 2005;48:372–80.
25. Enomoto N, Sakuma I, Asahina Y, et al. Comparison of full-length sequences of interferon-sensitive and resistant hepatitis C virus 1b. Sensitivity to interferon is conferred by amino acid substitutions in the NS5A region. J Clin Invest. 1995;96:224–30.
26. Enomoto N, Sakuma I, Asahina Y, et al. Mutations in the nonstructural protein 5A gene and response to interferon in patients with chronic hepatitis C virus 1b infection. N Engl J Med. 1996;334:77–81.
27. Shirakawa H, Matsumoto A, Joshita S, et al. Pretreatment prediction of virological response to peginterferon plus ribavirin therapy in chronic hepatitis C patients using viral and host factors. Hepatology. 2008;48:1753–60.
28. Oze T, Hiramatsu N, Yakushijin T, et al. Indications and limitations for aged patients with chronic hepatitis C in pegylated interferon alfa-2b plus ribavirin combination therapy. J Hepatol. 2011;54:604–11.
29. Kogure T, Ueno Y, Fukushima K, et al. Pegylated interferon plus ribavirin for genotype Ib chronic hepatitis C in Japan. World J Gastroenterol. 2008;14:7225–30.
30. Sezaki H, Suzuki F, Kawamura Y, et al. Poor response to pegylated interferon and ribavirin in older women infected with hepatitis C virus of genotype 1b in high viral loads. Dig Dis Sci. 2009;54:1317–24.
31. Ge D, Fellay J, Thompson AJ, et al. Genetic variation in IL28B predicts hepatitis C treatment-induced viral clearance. Nature. 2009;461:399–401.
32. Suppiah V, Moldovan M, Ahlenstiel G, et al. IL28B is associated with response to chronic hepatitis C interferon alpha and ribavirin therapy. Nat Genet. 2009;41:1100–4.
33. Tanaka Y, Nishida N, Sugiyama M, et al. Genome-wide association of IL28B with response to pegylated interferon alpha and ribavirin therapy for chronic hepatitis C. Nat Genet. 2009;41: 1105–9.

34. Miyase S, Haraoka K, Ouchida Y, et al. Randomized trial of peginterferon α-2a plus ribavirin versus peginterferon α-2b plus ribavirin for chronic hepatitis C in Japanese patients. J Gastroenterol. 2012;47:1014–21.
35. Minami T, Kishikawa T, Sato M et al. Meta-analysis: mortality and serious adverse events of peginterferon plus ribavirin therapy for chronic hepatitis C. J Gastroenterol. 2012. [Epub ahead of print].
36. Kobayashi M, Suzuki F, Akuta N et al. Relationship between SNPs in the *IL28B* region and amino acid substitutions in HCV core region in Japanese patients with chronic hepatitis C. Kanzo 2010;51:322–3.
37. Kurosaki M, Tanaka Y, Nishida N, et al. Pre-treatment prediction of response to pegylated -interferon plus ribavirin for chronic hepatitis C using genetic polymorphism in IL28B and viral factors. J Hepatol. 2011;54:439–48.
38. Thompson AJ, Muir AJ, Sulkowski MS, et al. Interleukin-28b polymorphism improves viral kinetics and is the strongest pretreatment predictor of sustained virologic response in genotype 1 hepatitis C virus. Gastroenterology. 2010;139:120–9.
39. Toyoda H, Kumada T, Tada T, et al. Predictive value of early viral dynamics during peginterferon and ribavirin combination therapy based on genetic polymorphisms near the IL28B gene in patients infected with HCV genotype 1b. J Med Virol. 2012; 84:61–70.
40. Marcellin P, Reau N, Ferenci P, et al. Refined prediction of week 12 response and SVR based on week 4 response in HCV genotype 1 patients treated with peginterferon alfa-2a (40KD) and ribavirin. J Hepatol. 2012;56:1276–82.
41. Sakai T.[PEG-interferonα-2a/ribavirin therapy for chronic hepatitis type 1b.] Kan Tan Sui 2006; 52:75–84. (in Japanese).
42. Perry CM, Jarvis B. Peginterferon-alpha-2a (40 kD): a review of its use in the management of chronic hepatitis C. Drugs. 2001; 61(15):2263–88.
43. Glue P, Fang JW, Rouzier-Panis R, Raffanel C, Sabo R, Gupta SK, et al. Pegylated interferon-alpha2b: pharmacokinetics, pharmacodynamics, safety, and preliminary efficacy data. Hepatitis C Intervention Therapy Group. Clin Pharmacol Ther. 2000;68(5): 556–67.
44. Formann E, Jessner W, Bennett L, et al. Twice-weekly administration of peginterferon-α-2b improves viral kinetics in patients with chronic hepatitis C genotype 1. J Viral Hepat. 2003;10: 271–6.
45. Aizaki H, Lee KJ, Sung VM, et al. Characterization of the hepatitis C virus RNA replication complex associated with lipid rafts. Virology. 2004;324:450–61.
46. Miyanari Y, Atsuzawa K, Usuda N, et al. The lipid droplet is an important organelle for hepatitis C virus production. Nat Cell Biol. 2007;9:1089–97.
47. Goldstein JL, Brown MS. Regulation of the mevalonate pathway. Nature. 1990;343:425–30.
48. Khorashadi S, Hasson NK, Cheung RC. Incidence of statin hepatotoxicity in patients with hepatitis C. Clin Gastroenterol Hepatol. 2006;4:902–7.

J Gastroenterol
DOI 10.1007/s00535-013-0830-1

ORIGINAL ARTICLE—LIVER, PANCREAS, AND BILIARY TRACT

New malignant grading system for hepatocellular carcinoma using the Sonazoid contrast agent for ultrasonography

Hironori Tanaka · Hiroko Iijima · Akiko Higashiura · Kazunori Yoh · Akio Ishii · Tomoyuki Takashima · Yoshiyuki Sakai · Nobuhiro Aizawa · Kazunari Iwata · Naoto Ikeda · Yoshinori Iwata · Hirayuki Enomoto · Masaki Saito · Hiroyasu Imanishi · Seiichi Hirota · Jiro Fujimoto · Shuhei Nishiguchi

Received: 24 July 2012 / Accepted: 1 May 2013

Abstract
Background The ultrasonography contrast agent Sonazoid provides parenchyma-specific contrast imaging (Kupffer imaging) based on its accumulation in Kupffer cells. This agent also facilitates imaging of the fine vascular architecture in tumors through maximum intensity projection (MIP). We examined the clinical utility of the malignancy grading system for hepatocellular carcinoma (HCC) using a combination of 2 different contrast-enhanced ultrasonography images.
Methods We studied 121 histologically confirmed cases of HCC (well-differentiated, 45; moderately differentiated, 70; poorly differentiated, 6). The results of Kupffer imaging were classified as (1) iso-echoic pattern or (2) hypo-echoic pattern. The MIP patterns produced were classified into one of the following categories: fine, tumor vessels were not clearly visualized and only fine vessels were visualized; vascular, tumor vessels were visualized clearly; irregular, tumor vessels were thick and irregular. Based on the combined assessment of Kupffer imaging and the MIP pattern, the samples were classified into 4 grades: Grade 1 (iso-fine/vascular), Grade 2 (hypo-fine), Grade 3 (hypo-vascular), and Grade 4 (hypo-irregular).
Results The distribution of moderately and poorly differentiated HCCs was as follows: Grade 1, 4 % (1/24); Grade 2, 52 % (15/29); Grade 3, 85 % (44/52); and Grade 4, 100 % (16/16). The grading system also predicted portal vein invasion in 72 resected HCCs: Grade 1, 0 % (0/4); Grade 2, 13 % (1/8); Grade 3, 23 % (11/48); and Grade 4, 67 % (8/12).
Conclusions This new malignant grading system is useful for estimation of histological differentiation and portal vein invasion of HCC.

Keywords Hepatocellular carcinoma · Contrast enhanced ultrasonography · Sonazoid · Malignant grade

H. Tanaka and H. Iijima contributed equally to this work.

H. Tanaka (✉) · H. Iijima · A. Higashiura · A. Ishii
Ultrasound Imaging Center, Hyogo College of Medicine,
1-1 Mukogawa-cho, Nishinomiya, Hyogo 663-8501, Japan
e-mail: hironori@hyo-med.ac.jp

H. Tanaka · H. Iijima · K. Yoh · T. Takashima · Y. Sakai · N. Aizawa · K. Iwata · N. Ikeda · Y. Iwata · H. Enomoto · M. Saito · H. Imanishi · S. Nishiguchi
Division of Hepatobiliary and Pancreas Disease, Department of Internal of Medicine, Hyogo College of Medicine,
1-1 Mukogawa-cho, Nishinomiya, Hyogo 663-8501, Japan

S. Hirota
Department of Surgical Pathology, Hyogo College of Medicine,
1-1 Mukogawa-cho, Nishinomiya, Hyogo 663-8501, Japan

J. Fujimoto
Division of Hepatobiliary and Pancreatic Disease, Department of External Medicine, Hyogo College of Medicine,
1-1 Mukogawa-cho, Nishinomiya, Hyogo 663-8501, Japan

Published online: 30 May 2013

Introduction

Hepatocellular carcinoma (HCC) represents the most common liver cancer and the third most common cause of cancer-related deaths [1, 2]. Knowledge of the histological grade of differentiation of HCC is useful in establishing a therapeutic strategy and in predicting therapeutic outcome, prognosis [3], and recurrence (especially in the case of internal metastases) [4]. However, tumor biopsy is the only strategy available for obtaining tumor tissue prior to therapy. Performing a biopsy of HCC has traditionally been avoided, because several cases of tumor seeding after biopsy have been reported [5, 6]. The risk of seeding is in

addition to the risk of complications, such as bleeding. Therefore, in order to determine the ideal therapeutic strategy, alternatives to biopsy are required.

The principal methods of diagnosis for HCC are imaging studies such as ultrasonography (US), computed tomography (CT), and magnetic resonance imaging (MRI). CT and MRI are superior to US in terms of objectivity. However, prediction of histological differentiation of HCC only by contrast-enhanced CT and MRI has limited effectiveness, because most classical HCCs are hyper-vascular in the arterial phase and hypo-vascular in the portal phase. Thus, it is difficult to distinguish histological differentiation by factors such as the vascular structure of the tumor.

Currently, there are only 2 US contrast agents available, Sonazoid and Levovist, which can be used for Kupffer imaging in the post-vascular phase (i.e., 10 min after injecting these agents). Bubbles made from Levovist, the first-generation US contrast agent, are very fragile and are easily collapsed by US emissions. Therefore, Kupffer imaging in the post-vascular phase using Levovist should be performed using a single sweep scan of the liver, which is insufficient for surveillance. However, Sonazoid, a second-generation US contrast agent, is a lipid-stabilized suspension of perfluorobutane and is composed of a hard shell containing bubbles. Due to this structure, microbubbles made from Sonazoid are chemically stable in blood vessels [7–9] and produce stable, non-linear oscillations in the low-power acoustic field. This feature allows Sonazoid to provide detailed perfusion features during imaging in the vascular phase and Kupffer imaging in the post-vascular phase, without bubble collapse. Specifically, Sonazoid is stable for at least 3 h after injection and, since the Sonazoid microbubbles are phagocytosed by liver Kupffer cells, this agent allows for multiple real-time scans. Malignant hepatic tumors, including HCC, contain few or no Kupffer cells, leading to an area clear of contrast material or a perfusion defect in Kupffer imaging. Therefore, perfusion defects seen on Kupffer imaging and the degree of histological malignancy of HCC are correlated [10–12]. Moderately or poorly differentiated HCC requires prompt therapy and Kupffer imaging has been a key imaging modality for the estimation of these histologic grades.

Moreover, using maximum intensity projection (MIP) [13], this type of contrast-enhanced ultrasonography (CEUS) could enable visualization of the fine vascular architecture in tumors, which also has been correlated with the histological differentiation of HCC [14]. The MIP pattern is an image that takes advantage of Sonazoid CEUS characteristics, such as high time and spatial resolution.

Hence, in comparison with other imaging modalities, these 2 imaging techniques, Kupffer imaging and MIP, could provide more relevant information for estimating the malignant grade of HCC. In this study, we examined the clinical utility of the malignant grading system for HCC using a combination of 2 different CEUS images, namely, Kupffer imaging and the MIP pattern.

Methods

Patients

We studied 116 patients with histologically confirmed HCC who were admitted to our institution between January 2008 and October 2010. Eighty patients were male and 36 were female, with a mean age of 69.9 years (range 38–92 years). Most of the 116 patients had a history of chronic liver disease, including hepatitis C virus (HCV) infection in 79 (68.1 %) patients and hepatitis B virus (HBV) infection in 14 (12.1 %) patients. Of the 116 patients included, 23 (19.8 %) were negative for both HCV and HBV. For the 23 patients that were negative for both viral markers, 13 (11 %) patients had alcoholic liver disease, 2 (2 %) patients had autoimmune hepatitis (AIH), 1 (1 %) patient had non-alcoholic steatohepatitis (NASH), and 7 (6 %) patients had cryptogenic hepatitis.

Liver specimens of 72 tumors (obtained from 71 patients who underwent partial hepatectomy) were analyzed in this study. The liver specimens obtained from 71 patients showed 34 patients with cirrhosis and the remaining 37 patients with chronic hepatitis. Presence of portal vein tumor invasion in these resected tumors was diagnosed by histological examination. An additional 49 tumors, obtained by 21-gauge needle core biopsy (Majima needle, Top Surgical Manufacturing, Tokyo, Japan) from 45 patients, were also evaluated for validation of the system. HCCs with regions of varying histological grades were classified as belonging to the predominating histological characteristic. The degree of differentiation was determined according to the International Working Party classification [15]. The final histological diagnoses of the 121 HCCs were as follows: 45 (37 %) well-differentiated, 70 (58 %) moderately differentiated, and 6 (5 %) poorly differentiated. This study was approved by the institutional ethics review board of Hyogo College of Medicine, Hyogo, Japan and all patients provided informed consent.

Sonologists

Two sonologists from our institution, with 20 (HT) and 30 (HI) years of experience in liver US imaging, were involved in this retrospective study. Each sonologist had at least 10 years of experience in microbubble contrast-enhanced US of the liver. They were aware of the patients' clinical histories and were blinded to the biopsy results.

Contrast-enhanced US study

The intravenously injected sonographic contrast agent, Sonazoid (Daiichi Sankyo, Tokyo, Japan; GE Healthcare, Little Chalfont, UK), was used in all studies. The suspension was prepared by vigorously shaking the powder with 2 mL of sterile water for 5–10 s. After the suspension was allowed to stand for 2 min to achieve equilibrium and the dissolution of large bubbles, the suspension was injected into an antecubital vein through a 21-gauge cannula at a speed of 1 mL/s and immediately flushed with 5–10 mL of normal saline.

US equipment included SSA-770A, SSA-790A, and TUS-A500 (Aplio; Toshiba Medical Systems, Tokyo, Japan) with a 3.75-MHz convex transducer (PSK-375BT). The imaging mode was wideband harmonic imaging (commercially called pulse subtraction) with transmission and reception frequencies of 3.75 and 7.5 MHz, respectively. When a suspected lesion was identified, CEUS was performed with the focus depth beyond the lesion of interest using the following settings: frame rate, 15 fps and dynamic range, 35 dB. A low mechanical index (MI) (0.16–0.30) was selected to avoid the disruption of microbubbles.

The region of interest was observed continuously for approximately 3 min from the time of injection. The arterial phase was timed for 45 s after completion of the flash. Approximately 20 min after the injection via the peripheral venous line, the liver was scanned again to observe Kupffer imaging (Fig. 1). Arterial-phase findings and Kupffer imaging were classified as follows: (1) hyper-echoic pattern, (2) iso-echoic pattern, and (3) hypo-echoic pattern.

After the Kupffer imaging was acquired, an MIP pattern was evaluated by reinjection of Sonazoid using micro-flow imaging (MFI), as was introduced by Sugimoto et al. [14]. Briefly, the maximum-hold processing started just after the burst scan. The burst scan consisted of high-MI (1.3–1.6) scanning of 5 frames. Low-MI (0.16–0.30) scanning was started again, just after the MI burst scanning, to visualize fresh microbubble contrast agent flowing into the scanning volume. The maximum intensity holding sequence was started simultaneously with flash replenishment low-MI imaging, which maintained maximum brightness on each pixel and was displayed as a persistent vision. The accumulation time for each MFI sequence was 10–15 s, depending on the perfusion of the target tissue.

MIP classification

The MIP pattern was classified into 1 of the following 3 patterns: (1) fine pattern: where tumor vessels were not clearly visualized and only fine vessels were visualized; (2) vascular pattern: where tumor vessels were visualized clearly; and (3) irregular pattern: where tumor vessels were thick and irregular (Fig. 1). The "tumor vessels" were defined as the vascular pattern in which vessels were obvious to the surrounding fifth or sixth branches. In cases where the vascular pattern was similar to that of the surrounding vessels, the tumor was classified as fine pattern. For accurate diagnose of the MIP pattern, the entire tumor was observed in vascular phase and the most suitable cross-sectional direction was chosen to enable identification of important signs of vascular and irregular patterns.

Malignant grading system

The combination of Kupffer imaging and MIP patterns classified HCCs into 4 grades: Grade 1 (iso-fine/vascular),

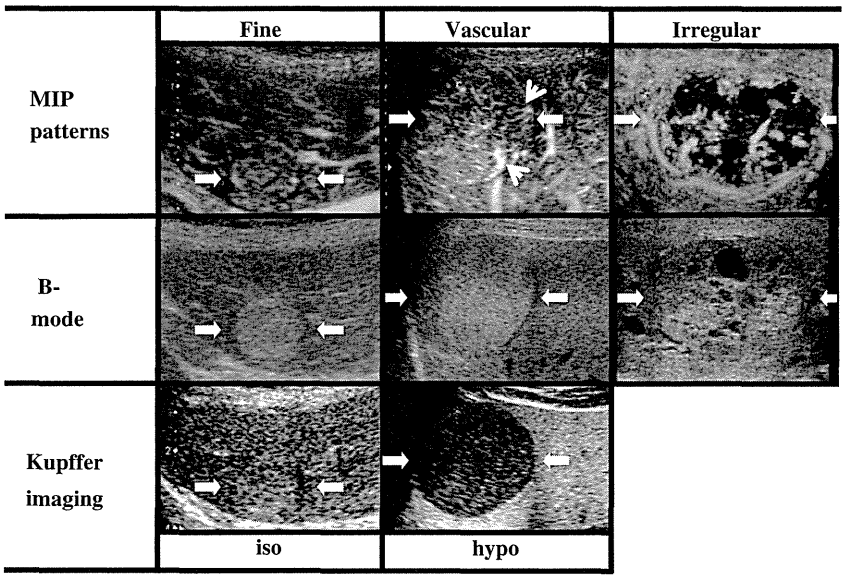

Fig. 1 Classification of MIP and Kupffer imaging. The MIP pattern is classified as 1 of the following 3 patterns: (1) fine pattern: where tumor vessels were not clearly visualized and only fine vessels were visualized; (2) vascular pattern: where tumor vessels were visualized clearly; and (3) irregular pattern: where tumor vessels were thick and irregular. *Small arrows* in "vascular" category of MIP patterns show tumor vessels of vascular pattern. Kupffer imaging is classified as 1 of following 2 patterns: (1) iso-echoic pattern, (2) hypo-echoic pattern

Grade 2 (hypo-fine), Grade 3 (hypo-vascular), and Grade 4 (hypo-irregular).

Statistical analysis

In the case of categorical variables, statistical analysis was performed using the Fisher's exact test. The Kruskal–Wallis H test was used for continuous variables. The Tukey–Kramer honestly significant difference was used for multiple comparisons. Relationships among the clinical parameters, such as malignant grade, tumor size, portal vein invasion, and histological differentiation were analyzed using Spearman's rank correlation coefficient. Unless otherwise noted, all data are presented as mean ± SD. $P < 0.05$ was considered statistically significant. The statistical analysis was performed with the JMP 8 (SAS Institute Inc., Cary, NC, USA).

Results

Arterial phase of HCCs and Kupffer imaging of HCCs

When compared with the adjacent liver tissue, 68 (94 %) lesions showed a hyper-echoic pattern and 4 (6 %) lesions showed an iso-echoic pattern during the arterial phase. As the degree of histological differentiation of HCC decreased, tumor hyper-vascularity increased: well-differentiated, 80 % (8/10); moderately differentiated, 96 % (54/56); and poorly differentiated, 100 % (6/6) (Table 1). Kupffer imaging of HCC according to histological differentiation showed the opposite tendency in that tumor hypo-intensity increased as the degree of histological differentiation of HCC decreased [well-differentiated, 60 % (6/10); moderately differentiated, 98 % (55/56); and poorly differentiated, 100 % (6/6)]. In Kupffer imaging, a hypo-echoic pattern was significantly larger in moderately or poorly differentiated HCCs, compared to well-differentiated HCCs ($P < 0.001$).

Table 1 Correlations between histological differentiated and patterns of contrast enhanced ultrasonography

	n	Arterial phase			Kupffer phase		
		Iso	Hyper	P^a	Iso	Hypo	P^b
Well	10	2	8	0.090	4	6	<0.001
Mod	56	2	54		1	55	
Poor	6	0	6		0	6	
Total	72	4	68		5	67	

Well Well differentiated HCC, *mod* moderately differentiated HCC, *poor* poorly differentiated HCC

[a] Proportion of hyper in arterial phase (well vs. mod/poor)

[b] Proportion of hyper in arterial phase (well vs. mod/poor)

Relationship between MIP patterns and histological differentiation or CEUS findings

In this study, intratumoral vessels of 72 tumors were clearly delineated using MIP. The vascular architecture of the tumors was as follows: fine, 12 (17 %); vascular, 48 (67 %); and irregular, 12 (17 %). Correlations between the MIP patterns and CEUS findings are presented in Fig. 2a, b. Most cases were hyper-echoic pattern in arterial phase (94 %) and hypo-echoic pattern in Kupffer imaging (93 %) and it was difficult to classify the MIP patterns using the CEUS patterns. Next, the correlations between the MIP patterns and histological differentiation were examined (Fig. 2c). We observed that 50 % (5/10) of well-differentiated HCCs showed a Fine pattern and 77 % (43/56) of moderately differentiated HCCs showed a vascular pattern, while the all poorly differentiated HCCs showed an irregular pattern. Furthermore, the irregular pattern was found only in moderately and poorly differentiated HCCs (Fig. 2c).

Histological differentiation and CEUS malignant grading system

As shown in Fig. 3a, Grade 1 included no moderately differentiated HCC tumors. In contrast, all poorly differentiated HCCs were Grade 4. This tendency became more clear when we considered the relationship among all 121 nodules, including biopsy-confirmed HCCs. There was a close relationship between malignant grade and histologic differentiation ($r = 0.712$, $P < 0.0001$). Thus, this grading system could predict moderately and poorly differentiated HCCs: Grade 1, 4 % (1/24); Grade 2, 52 % (15/29); Grade 3, 85 % (44/52); and Grade 4, 100 % (16/16).

Tumor size and malignant grading system

When evaluating tumor size according to the grading system, mean tumor size increased: Grade 1, 18.2 ± 4.7 mm; Grade 2, 16.6 ± 4.2 mm; Grade 3, 30.6 ± 14.7 mm; and Grade 4, 53.2 ± 21.3 mm ($r = 0.590$, $P < 0.001$). Tumor sizes were similar between Grades 1 and 2, but there was a greater increase in size between Grades 3 and 4 (Fig. 4a).

Portal vein invasion and clinical parameters

When portal vein invasion was compared with 72 resected HCCs, all HCCs with portal vein invasion were high-echoic pattern in arterial phase and hypo-echoic pattern in Kupffer imaging. There were only 4 (8 %) HCCs without portal vein invasion that showed an iso-echoic pattern

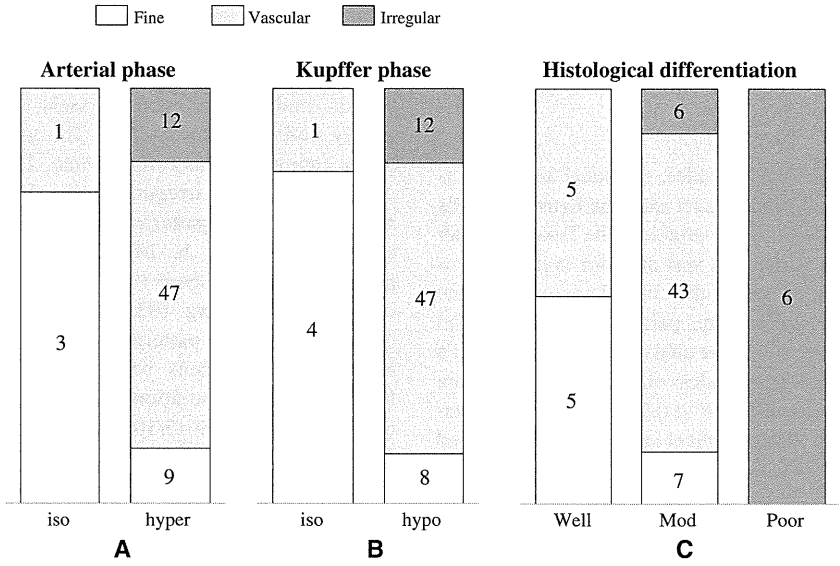

Fig. 2 Correlation between maximum intensity projection (MIP) patterns and contrast-enhanced ultrasonography (CEUS) findings or histological differentiation of hepatocellular carcinoma (HCC). **a** In the arterial phase, most HCCs depicted as an iso-echoic pattern showed a fine pattern and most hyper-echoic HCCs were vascular. All HCCs depicted as irregular showed a hyper-echoic pattern. **b** Kupffer imaging. In a similar fashion, most HCCs with iso-echoic patterns showed a fine pattern and most with hypo-echoic patterns were vascular. All HCCs depicted as irregular showed a hyper-echoic pattern. **c** In histological differentiation, 77 % (43/56) of moderately differentiated HCCs showed a vascular pattern and the irregular pattern was found only in moderately and poorly-differentiated HCCs

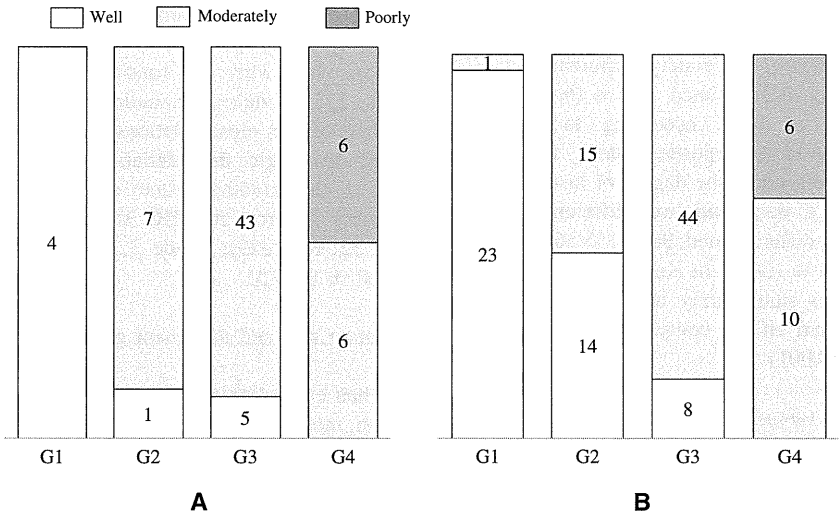

Fig. 3 Correlations between malignant grading system and HCC differentiation. The malignant grading system classified HCC into 4 grades. The combination of Kupffer imaging and MIP patterns classified HCC into 4 grades: Grade 1 (iso-fine/vascular), Grade 2 (hypo-fine), Grade 3 (hypo-vascular), and Grade 4 (hypo-irregular). **a** 72 resected HCCs. **b** All 121 HCCs, including the 72 resected HCCs and 49 HCCs diagnosed by biopsy specimen. Most malignant Grade 1 (G1) HCCs were well-differentiated and there were no well-differentiated HCCs in Grade 4 (G4). Poorly differentiated HCCs were identified only in G4. The proportions of moderately or poorly differentiated HCCs increased with increasing malignant grade. The close relationship between malignant grade and histological differentiation was confirmed, especially in all 121 HCCs ($r = 0.755$, $P < 0.0001$)

both in arterial phase and Kupffer imaging and almost all echo patterns of HCCs without portal vein invasion were hyper-echoic in both arterial phase and hypo-echoic in Kupffer imaging (Fig. 5a, b). Hence, using only CEUS patterns, it is difficult to distinguish the HCCs with portal vein invasion. However, the rates of positive portal vein

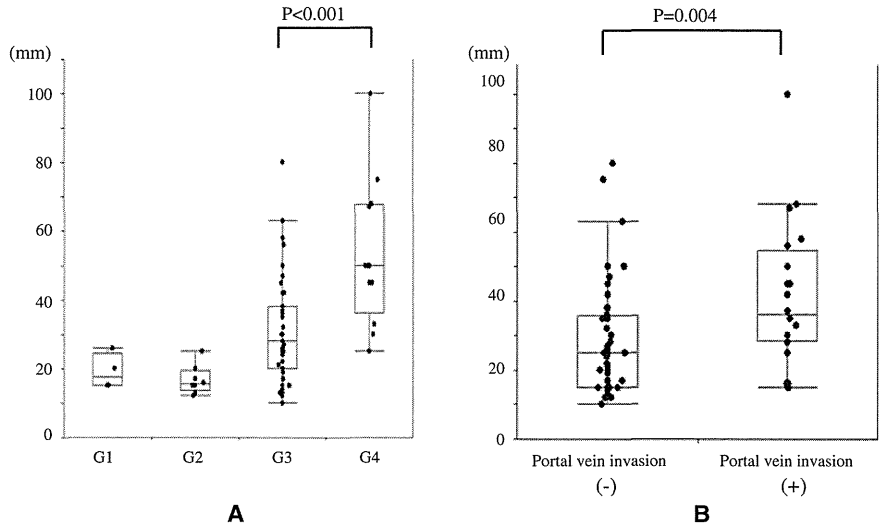

Fig. 4 Correlations between tumor size and malignant grading system and portal vein invasion. **a** Correlation with malignant grading system. Tumor sizes were similar between Grades 1 and 2, but there was a greater increase in size between Grades 3 and 4. **b** Correlation with portal vein invasion. Although HCCs positive for portal vein invasion were larger than negative HCCs, discriminating the positive cases only using tumor size was difficult

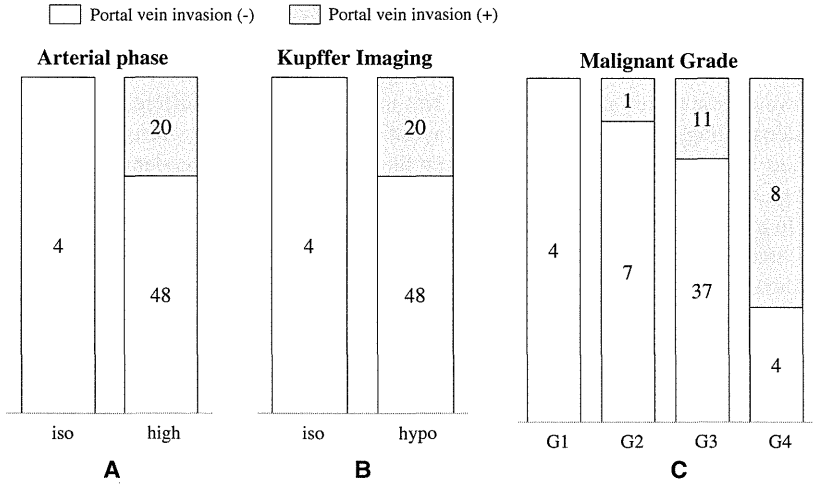

Fig. 5 Correlations between portal vein invasion and CEUS parameters. Arterial phase (**a**) and Kupffer imaging (**b**) showed the same patterns when these parameters were analyzed with portal vein invasion. Most cases, including all portal vein-positive HCCs, were hyper-echoic in the arterial phase and hypo-echoic in Kupffer imaging. Portal vein invasion-positive rates increased with increasing malignant grade (**c**)

invasion increased with the CEUS malignant grade: Grade 1, 0 % (0/4); Grade 2, 13 % (1/8); Grade 3, 23 % (11/47); and Grade 4, 67 % (8/12) (Fig. 5c). This correlation was closer ($r = 0.385$, $P < 0.001$) than the correlation between portal vein invasion and tumor size ($r = 0.359$, $P = 0.002$).

The significance of the tumor markers, such as AFP and DCP, were also evaluated for their ability to detect portal vein invasion (Fig. 6). However, no correlation was demonstrated between tumor markers and portal vein invasion.

Discussion

This study proposes a new malignant grading system that incorporates two key features of CEUS and demonstrates a strong correlation between this new grading system and histological differentiation of HCC. Both Kupffer imaging and MIP are unique imaging techniques that utilize characteristics of Sonazoid CEUS. These images are difficult to obtain by other imaging modalities, such as CT or MRI. Detection of small HCCs by CT or MRI without contrast medium can be difficult and use of contrast media for both

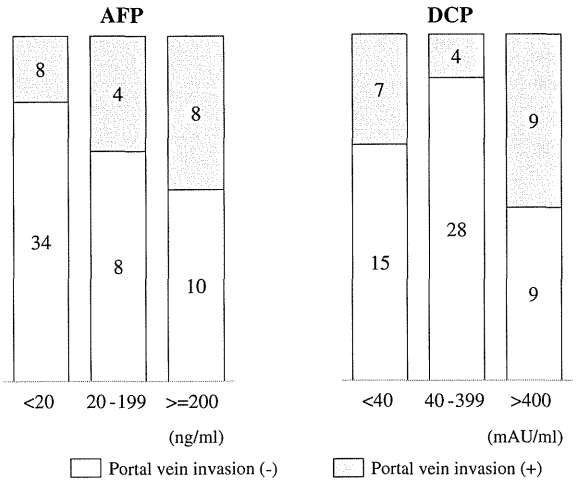

Fig. 6 Correlations between portal vein invasion and tumor markers. **a** Alpha-fetoprotein (AFP). **b** Des-gamma carboxyprothrombin (DCP). No correlation was demonstrated between tumor markers and portal vein invasion

CT and MRI is sometimes restricted by renal function and allergy. Hence, our new malignant grading system using CEUS, which is associated with little or no side effects, is of particular value. Notably, it is difficult to estimate the degree of malignancy using only an imaging technique. However, the term "malignant grade" was used here to aid understanding, similar to the use by Hayashi et al., in their report indicating the correlation between blood supply and progression of hepatocellular nodules [16].

In addition, ultrasonography yielded several details such as size, shape, and internal echo pattern of tumors. Although tumor size is also an important factor for evaluating the differentiation of HCC, it is difficult to distinguish the histological differentiation especially in small nodules. This tendency was confirmed in our results. Although tumor sizes in Grades 1 and 2 were similar (Grade 1, 18.2 ± 4.7 mm; Grade 2, 16.6 ± 4.2 mm), histological differences were identified between malignant Grades 1 and 2 ($P = 0.001$) (Fig. 3a). As just described, it is difficult to distinguish histological differentiation only by tumor size. US also demonstrated characteristic findings in internal echo patterns. Nevertheless, internal echo patterns were not easily distinguishable and, in this way, the objectivity of these results was limited.

Using the Sonazoid contrast medium, additional arterial phase, Kupffer imaging, and MIP patterns imaging were also obtained. This study showed a definite correlation between each of these findings and histological differentiation, although no significant difference was achieved only in arterial phase due to the small population size. Therefore, all these results are of value. Kupffer imaging is a unique imaging technique that, since Levovist was discontinued, currently can only be accomplished using Sonazoid CEUS or super paramagnetic iron oxide magnetic resonance images (SPIO-MRI). HCC intensity changes on Kupffer imaging according to the progression of histological differentiation [10, 11]. For example, the tumor intensity, on Kupffer imaging by Sonazoid CEUS, changes from an iso- to a hypo-echoic pattern as the histological differentiation changes from well- to moderately differentiated HCC. Kupffer imaging can also be obtained by SPIO-MRI. However, SPIO-MRI cannot obtain vascular imaging and the resolution is inadequate.

MIP is a CEUS modality in which the imaging is based on an accumulation of images. MIP combines the flash-replenishment sequence with maximum-holding image processing to distinctly delineate the blood vessels in tissue [14]. HCC is known to undergo changes in vascular structure as it progresses. MIP can help visualize this fine vascular structure without angiography of the liver. In this study, half of the well-differentiated HCCs demonstrated fine patterns. The proportion of fine patterns of well-differentiated HCC was higher (73 %), when analyzed with all 121 HCCs. In contrast, all 12 patients with irregular patterns had either moderately or poorly differentiated HCC and all poorly differentiated HCCs demonstrated irregular patterns (Fig. 2c). The prognosis associated with these tumors was poor. All 6 patients with moderately differentiated HCC with an irregular pattern also had a recurrence within 2 years (data not shown). Moreover, the moderately differentiated HCCs could be further divided into a less malignant group (fine pattern) and a more malignant group (irregular pattern) using our grading system. Some of the CEUS results showed similar tendencies in the correlation with histological differentiation. For example, both arterial phase and Kupffer imaging showed similar patterns with respect to the degree of histological differentiation (Table 1). These results indicate that combining these 2 imaging modalities would yield little additional information. In this study, we did not combine arterial phase findings and MIP patterns, although this combination would allow for shortening the time of examination. These techniques were not combined because both reflect the vascularity of a HCC and contain similar information and because the arterial phase evaluation would have to be limited to 20 s, causing the optimal moment for appropriate assessment to be missed in some cases. In contrast, Kupffer phase imaging could be assessed repeatedly from various angles and serves as an indispensable phase of the CEUS examination. Thus, the combination of Kupffer imaging and MIP patterns would be the most sensible and complementary method for evaluating the histological differentiation of HCC. For example, 7 moderately differentiated HCCs with Fine patterns were indistinguishable from well-differentiated HCCs only using

MIP patterns (Fig. 3a). All of these tumors were of malignant Grade 2 and could be distinguished by adding Kupffer imaging.

Our grading system was also correlated with portal vein invasion ($r = 0.385$). Tumor size is also one of the important factors for the prediction of portal vein invasion and was correlated with portal vein invasion in this study ($r = 0.359$). However, AFP and DCP, as the representative tumor markers for HCC, also did not show correlations with portal vein invasion in this study (AFP, $r = 0.050$; DCP, $r = 0.203$). Thus, both our malignant grade and tumor sizes are important for the prediction of the portal vein invasion. Since some cases with small HCC and portal vein invasion exist, our malignant grade could be expected to identify these cases with small portal vein invasion.

Sugimoto et al. [14] reported the classification of HCC using MIP patterns and the MIP pattern concept used in this study was similar to theirs in that the categories, fine, vascular, and irregular, are parallel to the normal or cotton, vascular, and dead wood categories used in the previous study. An advantage of our MIP classification is the simplicity of classification. If some irregular vessels can be detected, the case is classified as "irregular pattern". Similarly, if some tumor vessels thicker than the surrounding fifth or sixth branch can be detected, the case is classified as "vascular pattern". Other cases were classified into "fine pattern," including cases in which the difference between the tumor vessels and surrounding hepatic parenchyma could not be detected. In addition, the "cotton pattern" terminology could be misunderstood to indicate the classical contrast-enhanced pattern of a hemangioma [17, 18]. Furthermore, the term "dead wood" is associated with large HCCs. However, to the extent possible, a system should be able to detect irregular vessels in a small size. Therefore, the current MIP patterns were chosen in this study.

There are some limitations associated with this malignant grading system. First, it is possible that the grading system contains some bias due to tumor size. In this study, only resected cases were analyzed, because a sample taken by fine-needle biopsy may not always represent the majority histological characteristics of HCC, especially in nodule-in-nodule cases. As a result, the proportion of well-differentiated HCC cases was small. To address this limitation, our grading system was validated using 49 HCCs diagnosed by fine needle biopsy and ablated by radiofrequency ablation (Fig. 3b). This validation raised the stratification of our grading system and could indicate following association, an HCC grade of 1 or 3 indicates a well- or moderately differentiated HCC, respectively. An additional limitation of this study is objectivity, which is a problem inseparable from ultrasonography. However, the subjectivity of our MIP classification is minimized by the simplicity of classification, as previously described. A possible limitation of this MIP pattern was the possibility that key images could not be detected because only the two dimensional image of MIP patterns, but not the entire tumor, was detectable. Hence, these cases might be classified into a less malignant grade. However, misclassified cases could be minimized using the CEUS method introduced in "Methods".

This study was an exploratory study. Our dataset includes both early and advanced HCC and is therefore a true representation of daily clinical practice. Since the dataset was small, the focus was on the analysis of the value of the CEUS malignant grading system. Future studies are necessary to support an association between our malignant grading system and overall survival.

Conclusions

This malignant grading system for HCC, using a combination of Kupffer imaging and MIP pattern, could evaluate not only the histological differentiation of HCC but also portal vein invasion.

Conflict of interest Shuhei Nishiguchi received financial support from Chugai Pharmaceutical, MSD, Dainippon Sumitomo Pharma, Ajinomoto Pharma, and Otsuka Pharmaceutical. Hiroko Iijima received financial support from Chugai Pharmaceutical. Hiroyasu Imanishi received financial support from Chugai Pharmaceutical. The remaining authors have no conflict of interest.

References

1. El-Serag HB, Rudolph KL. Hepatocellular carcinoma: epidemiology and molecular carcinogenesis. Gastroenterology. 2007;132:2557–76.
2. Parkin DM, Bray F, Ferlay J, Pisani P. Global cancer statistics, 2002. CA Cancer J Clin. 2005;55:74–108.
3. Tamura S, Kato T, Berho M, Misiakos EP, O'Brien C, Reddy KR, et al. Impact of histological grade of hepatocellular carcinoma on the outcome of liver transplantation. Arch Surg. 2001;136:25–30 Discussion 31.
4. Kumada T, Nakano S, Takeda I, Sugiyama K, Osada T, Kiriyama S, et al. Patterns of recurrence after initial treatment in patients with small hepatocellular carcinoma. Hepatology. 1997;25:87–92.
5. Sakurai M, Okamura J, Seki K, Kuroda C. Needle tract implantation of hepatocellular carcinoma after percutaneous liver biopsy. Am J Surg Pathol. 1983;7:191–5.
6. Smith EH. Complications of percutaneous abdominal fine-needle biopsy. Review. Radiology. 1991;178:253–8.
7. Watanabe R, Matsumura M, Chen CJ, Kaneda Y, Ishihara M, Fujimaki M. Gray-scale liver enhancement with Sonazoid (NC100100), a novel ultrasound contrast agent; detection of hepatic tumors in a rabbit model. Biol Pharm Bull. 2003;26:1272–7.
8. Hagen EK, Forsberg F, Åksnes AK, Merton DA, Liu JB, Tornes A, et al. Enhanced detection of blood flow in the normal canine prostate using an ultrasound contrast agent. Invest Radiol. 2000;35:118–24.

9. Yao J, Teupe C, Takeuchi M, Avelar E, Sheahan M, Connolly R, et al. Quantitative 3-dimensional contrast echocardiographic determination of myocardial mass at risk and residual infarct mass after reperfusion: experimental canine studies with intravenous contrast agent NC100100. J Am Soc Echocardiogr. 2000;13:570–81.
10. Korenaga K, Korenaga M, Furukawa M, Yamasaki T, Sakaida I. Usefulness of Sonazoid contrast-enhanced ultrasonography for hepatocellular carcinoma: comparison with pathological diagnosis and superparamagnetic iron oxide magnetic resonance images. J Gastroenterol. 2009;44:733–41.
11. Imai Y, Murakami T, Yoshida S, Nishikawa M, Ohsawa M, Tokunaga K, et al. Superparamagnetic iron oxide-enhanced magnetic resonance images of hepatocellular carcinoma: correlation with histological grading. Hepatology. 2000;32:205–12.
12. Inoue T, Kudo M, Watai R, Pei Z, Kawasaki T, Minami Y, et al. Differential diagnosis of nodular lesions in cirrhotic liver by post-vascular phase contrast-enhanced US with Levovist: comparison with superparamagnetic iron oxide magnetic resonance images. J Gastroenterol. 2005;40:1139–47.
13. Wilson SR, Jang HJ, Kim TK, Iijima H, Kamiyama N, Burns PN. Real-time temporal maximum-intensity-projection imaging of hepatic lesions with contrast-enhanced sonography. Am J Roentgenol. 2008;190:691–5.
14. Sugimoto K, Moriyasu F, Kamiyama N, Metoki R, Yamada M, Imai Y, et al. Analysis of morphological vascular changes of hepatocellular carcinoma by microflow imaging using contrast-enhanced sonography. Hepatol Res. 2008;38:790–9.
15. Terminology of nodular hepatocellular lesions. International Working Party. Hepatology. 1995;22:983–93.
16. Hayashi M, Matsui O, Ueda K, Kawamori Y, Kadoya M, Yoshikawa J, et al. Correlation between the blood supply and grade of malignancy of hepatocellular nodules associated with liver cirrhosis: evaluation by CT during intraarterial injection of contrast medium. Am J Roentgenol. 1999;172:969–76.
17. Johnson CM, Sheedy PF, Stanson AW, Stephens DH, Hattery RR, Adson MA. Computed tomography and angiography of cavernous hemangiomas of the liver. Radiology. 1981;138:115–21.
18. Wen YL, Kudo M, Zheng RQ, Ding H, Zhou P, Minami Y, et al. Characterization of hepatic tumors: value of contrast-enhanced coded phase-inversion harmonic angio. Am J Roentgenol. 2004;182:1019–26.

J Gastroenterol
DOI 10.1007/s00535-013-0884-0

ORIGINAL ARTICLE—LIVER, PANCREAS, AND BILIARY TRACT

Thrombocytopenia in pegylated interferon and ribavirin combination therapy for chronic hepatitis C

Nobuhiro Aizawa · Hirayuki Enomoto · Tomoyuki Takashima · Yoshiyuki Sakai · Kazunari Iwata · Naoto Ikeda · Hironori Tanaka · Yoshinori Iwata · Masaki Saito · Hiroyasu Imanishi · Hiroko Iijima · Shuhei Nishiguchi

Received: 22 May 2013 / Accepted: 5 September 2013

Abstract
Background This study aimed to examine the therapeutic effect and prognostic indicators of pegylated interferon (PEG-IFN) and ribavirin (RBV) combination therapy in thrombocytopenic patients with chronic hepatitis C, hepatitis C virus (HCV)-related cirrhosis, and those who underwent splenectomy or partial splenic embolization (PSE).
Methods Of 326 patients with HCV-related chronic liver disease (252 with genotype 1b and 74 with genotype 2a/2b) treated with PEG-IFN/RBV, 90 were diagnosed with cirrhosis.
Results Regardless of the degree of thrombocytopenia, the administration rate was significantly higher in the splenectomy/PSE group compared to the cirrhosis group. However, in patients with genotype 1b, the sustained virological response (SVR) rate was significantly lower in the cirrhosis and the splenectomy/PSE groups compared to the chronic hepatitis group. No cirrhotic patients with platelets less than 80,000 achieved an SVR. Patients with genotype 2a/2b were more likely to achieve an SVR than genotype 1b. Prognostic factors for SVR in patients with genotype 1b included the absence of esophageal and gastric varices, high serum ALT, low AST/ALT ratio, and the major homo type of the IL28B gene. Splenectomy- or PSE-facilitated induction of IFN in patients with genotype 2a/2b was more likely to achieve an SVR by an IFN dose maintenance regimen. Patients with genotype 1b have a low SVR regardless of splenectomy/PSE. In particular, patients with a hetero/minor type of IL28B did not have an SVR.
Conclusions Splenectomy/PSE for IFN therapy should be performed in patients expected to achieve a treatment response, considering their genotype and IL28B.

Keywords IFN therapy · IL28B · Partial splenic embolization · Splenectomy · Thrombocytopenia

Introduction

Chronic hepatitis C is characterized by recurrent necrosis and regeneration in the setting of persistent inflammation, leading to progressive hepatic fibrosis, which increases the risk of carcinogenesis. In cirrhotic livers, cancer develops at a higher rate [1, 2]. However, after a virus has been removed by interferon (IFN) therapy, hepatic fibrosis can improve, and the incidence of liver cancer is subsequently reduced [3–5]. Therefore, to prevent fibrosis and liver carcinogenesis, virus elimination by antiviral therapies is paramount in advanced cases.

As an antiviral therapy for chronic hepatitis C, pegylated interferon (PEG-IFN) in combination with ribavirin (RBV) has resulted in remarkably favorable outcomes, with a sustained virological response (SVR) obtained in approximately 80 % of patients with genotypes 2 and 3 and, more impressively, 40–50 % of patients with genotype 1 and a refractory high viral load [6–9].

As fibrosis progresses, however, the therapeutic effect of antivirals diminishes. Studies have reported that the effect of PEG-IFN/RBV combination therapy for liver cirrhosis characterized by progressive fibrosis was exceedingly poor,

N. Aizawa · H. Enomoto (✉) · T. Takashima · Y. Sakai · K. Iwata · N. Ikeda · H. Tanaka · Y. Iwata · M. Saito · H. Imanishi · H. Iijima · S. Nishiguchi
Division of Hepatobiliary and Pancreatic Diseases, Department of Internal Medicine, Hyogo College of Medicine, 1-1 Mukogawa-cho, Nishinomiya, Hyogo 6638501, Japan
e-mail: enomoto@hyo-med.ac.jp

Published online: 25 September 2013

with the SVR rates 14–27 % in patients with genotype 1 and 33–56 % in patients with genotypes 2 and 3 [10–12].

It is very important to maintain the IFN dose as the administration rate in addition to the presence of fibrosis greatly influences the therapeutic effect [13, 14]. However, it can be difficult to maintain the IFN dose in patients with cirrhosis complicated by hypersplenism. Thrombocytopenia from hypersplenism can develop and/or be exacerbated following IFN therapy, making ongoing therapy problematic. In addition, the induction of IFN therapy may be difficult in some of these patients [15, 16]. Hence, to address cytopenias including thrombocytopenia, splenectomy or partial splenic embolization (PSE) can be performed for hepatitis C virus (HCV)-related cirrhosis with hypersplenism [17–23]. However, the therapeutic effect and long-term safety and efficacy of such treatment have not been sufficiently examined.

Recently, studies have reported that the interferon sensitivity-determining region (ISDR) and amino acid substitutions of core 70 and core 91 in the core region of HCV are important prognostic indicators of IFN's therapeutic effect. Furthermore, the therapeutic effect rate of IFN depends on the genetic polymorphism of IL28B [24–29].

The objectives of this study were to examine the therapeutic effect and associated prognostic indicators of PEG-IFN/RBV therapy in thrombocytopenic patients with chronic hepatitis and HCV-related cirrhosis and those who underwent splenectomy or PSE.

Methods

Patients

This study was approved by the Ethics Committee of the Hyogo College of Medicine (approval no. 92, 391) and adhered to the guidelines of the Declaration of Helsinki. Written informed consent was obtained from all patients after the objectives and nature of the study had been discussed.

Between January 2005 to 2012, 326 patients with HCV-related chronic liver disease who were started on PEG-IFN/RBV combination therapy and followed at the Hyogo College of Medicine Hospital were enrolled in the study (Fig. 1).

Twenty-six patients were diagnosed with cirrhosis macroscopically when they underwent splenectomy in our hospital. Of 45 patients with esophageal and gastric varices and diagnosed with cirrhosis on abdominal imaging, two underwent splenectomy in other hospitals, and one underwent PSE prior to IFN therapy.

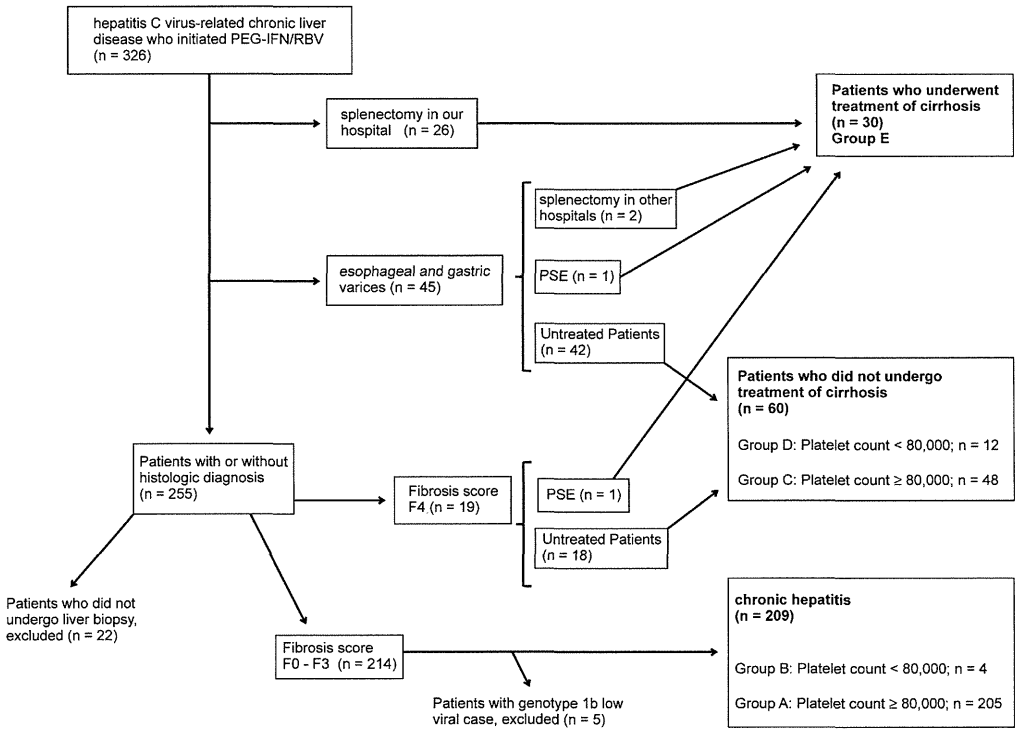

Fig. 1 Flow diagram of study patients

Of the remaining 255 patients, 22 patients who did not undergo liver biopsy were excluded from the study, 233 patients underwent a liver biopsy, and 19 were diagnosed to have cirrhosis histologically. One of the 19 patients subsequently underwent PSE prior to IFN therapy. In total, there were 90 patients diagnosed with cirrhosis in this study. The 30 patients with cirrhosis who underwent splenectomy or PSE (treated cirrhosis group) were compared to the 60 patients who did not have either procedure (untreated cirrhosis group).

Of the 233 patients who had a liver biopsy, 214 did not have histological diagnosis of cirrhosis. Five patients with genotype 1b low viral load (HCV-RNA <100 K IU/ml) in the chronic hepatitis group were excluded from this study because there were no patients with genotype 1b low viral load in the corresponding cirrhosis group.

There were 43 patients (4, 12, and 27 patients in group B, D, and E, respectively) with a platelet count of less than 80,000 prior to the initiation of IFN therapy. They were fully informed aboout the expected benefits and associated risks of splenectomy or PSE. Twenty-five consented to splenectomy, while another two chose to undergo PSE prior to IFN therapy.

One patient with a platelet count of slightly more than 80,000 requested to undergo splenectomy. Therefore, we initiated IFN therapy in this patient and considered the patient in the treated group analysis in this study. With regard to the two patients who had already undergone splenectomy for portal hypertension in other hospitals, although their lowest platelet counts prior to splenectomy were unknown, they were nevertheless also included in the treated group.

Patients with uncontrolled ascites, liver cancer, esophageal, and/or gastric varices requiring treatment and those who underwent liver transplantation were excluded from this study. Patients with positive hepatitis B virus surface antigen, positive human immunodeficiency virus antigen, or other hepatic disorders (e.g., primary biliary cirrhosis or autoimmune hepatitis) were also excluded.

Table 1 shows the characteristics of 299 patients (groups A, B, C, D, and E; see Fig. 1) prior to IFN therapy. Blood work before splenectomy or PSE is also provided for those who underwent these procedures.

Treatment for hepatitis C virus

Peginterferon alpha-2a (Pegasys®; Chugai, Japan) was administered to 113 patients, and 186 were treated with peginterferon alpha-2b (Pegintron®; MSD, Japan). The basic dose each week was either 180 μg of peginterferon alpha-2a or 1.0–1.5 μg/kg of peginterferon alpha-2b. RBV combination therapy was also given to all patients and was administered orally each day at a basic dose depending on body weight (<60 kg, 600 mg; 60–80 kg, 800 mg; >80 kg, 1,000 mg).

Patients with genotype 1b and 2a/2b were treated for 48 and 24 weeks, respectively. Based on the patient request, 106 with genotype 1b were treated for 50–90 weeks, and 34 with genotype 2a/2b were treated for 30–72 weeks.

Laboratory and histological tests

The amount of HCV was measured by COBAS AMPLICOR HCV MONITOR test, version 2.0 (detection range 6–5000 K IU/ml; Roche Diagnostics, Branchburg, NJ, USA). Qualitative analysis was performed using COBAS AMPLICOR HCV test, version 2.0 (lower limit of detection 50 IU/ml; Roche Diagnostics). For patients who started IFN therapy after January 2008, the amount of HCV was measured by COBAS TaqMan HCV test (Roche Diagnostics). Six months after completing treatment, patients with negative HCV RNA were considered to have an SVR.

ISDR, Core 70, and Core 91 were measured by the direct sequencing method, as previously reported [23, 24]. The IL28B gene (rs 8099917) was measured using the TaqMan probe method, as previously reported [25].

Histological assessment of fibrosis was scored using the METAVIR scoring system: F0, no fibrosis; F1, mild fibrosis or portal fibrosis without septa; F2, moderate fibrosis or few septa; F3, severe fibrosis or numerous septa without cirrhosis; F4, cirrhosis.

Study analysis

We recently reported a nationwide survey in Japan regarding splenectomy/PSE for interferon treatment targeting HCV-related chronic liver disease in patients with low platelet counts. We found that many patients with platelet counts <80,000 were treated with a reduced dose of IFN, at which the SVR rate was predicted to be low [30]. Therefore, we classified the patients with platelet counts of 80,000 in the present study. Before IFN therapy, patients with chronic hepatitis who had the lowest platelet count of at least 80,000 were assigned to group A, whereas those with a platelet count of less than 80,000 were placed in group B. Patients with liver cirrhosis who had platelet counts of at least 80,000 before IFN therapy were assigned to group C, whereas those with platelet counts of less than 80,000 before IFN therapy were placed in group D. Group E comprised patients who received IFN therapy after splenectomy or PSE (Fig. 1). The IFN administration rate was examined according to each group. Treatment was discontinued in patients who failed to demonstrate virus-negative results by 24 weeks. Therefore, the IFN dose was evaluated using the dose administered until 24 weeks. The

Table 1 Baseline characteristics of the patients

Factor	Value (range or number)		
	Chronic hepatitis ($n = 209$)	Liver cirrhosis ($n = 60$)	PSE or splenectomy ($n = 30$)
Sex (male/female) (cases)	90/119	35/25	16/14
Mean age/range (years)	57.9 ± 11.2	62.7 ± 9.2	61.0 ± 7.1
White blood cells (/mm^3)	4,648.8 ± 1,613.8	4,068.3 ± 1,156.2	3,410.4 ± 1,268.3[a]
Hemoglobin (g/dl)	13.8 ± 1.5	13.2 ± 1.6	12.5 ± 2.2[a]
Platelet count ($\times 10^4$/mm^3)	16.2 ± 4.9	11.2 ± 3.0	6.0 ± 1.4[a]
AST (IU/l)	47.2 ± 32.4	77.2 ± 47.1	58.0 ± 24.2[a]
ALT (IU/l)	57.9 ± 51.8	82.3 ± 58.9	54.8 ± 24.9[a]
AST/ALT	0.94 ± 0.29	1.01 ± 0.25	1.12 ± 0.30[a]
Total bilirubin (mg/dl)	0.8 ± 0.3	0.9 ± 0.4	1.2 ± 0.5[a]
Albumin (g/dl)	4.1 ± 0.3	3.8 ± 0.4	3.7 ± 0.5[a]
PT percentage activity (%)	94.6 ± 10.0	83.5 ± 8.9	80.6 ± 13.2[a]
Associated esophageal varices (cases) (present/absent)	0/209	42/18	18/12
History of treatment for HCC (cases) (with or without)	9/200	19/41	6/24
Previous treatment of IFN (cases) with or without)	81/128	30/30	24/6
HCV genotype (1b/2a/2b/2a + 2b/2a or 2b) (cases)	153/31/22/3/0	50/6/3/0/1	25/4/1/0/0
HCV-RNA (KIU/ml)			
100 ≤ HCV-RNA < 1,000 KIU/ml (cases)	64	19	10
≥1,000 KIU/ml (cases)	145	41	20
Amino acid substitutions in the HCV genotype 1b	($n = 153$)	($n = 50$)	($n = 25$)
Core aa 70 [arginine/glutamine (histidine)/ND]	92/49/12	22/26/2	12/13/0
Core aa 91 (leucine/methionine/ND)	95/46/12	35/13/2	19/6/0
ISDR of NS5A in the HCV genotype 1b	($n = 153$)	($n = 50$)	($n = 25$)
(Wild type/non-wild type/ND)	117/23/13	38/9/3	22/3/0
Genetic variation near IL28B gene(rs 8099917) in patients with genotype 1b	($n = 153$)	($n = 50$)	($n = 25$)
(TT/TG/GG/ND)	81/42/4/26	29/17/1/3	16/9/0/0

AST Aspartate aminotransferase, *ALT* alanine aminotransferase, *AST/ALT* aspartate aminotransferase/alanine aminotransferase ratio, *ND* not determined

[a] We excluded two patients who had already undergone splenectomy in other hospitals because we could not obtain their data before splenectomy

normal dose each week was either 180 μg of peginterferon alpha-2a or 1.5 μg/kg of peginterferon alpha-2b. The actual dose rate was evaluated as <50, 50–80, and 80 % or more of the normal dose.

The SVR rate in each group was examined according to genotype. In group E, biochemical tests before and after splenectomy or PSE were compared.

In the liver cirrhosis groups, the factors contributing to SVR were examined in those with genotype 1 and a high viral load.

Statistical analysis

Baseline data are expressed as mean ± SD or median values. Virologic response was evaluated using the full analysis set (FAS). In patients who underwent splenectomy or PSE, pre- and postoperative blood work was compared using the Wilcoxon signed-rank test. The IFN administration rate was compared using the chi-square test.

To compare SVRs, the patient characteristics were compared using the Mann-Whitney *U* test, Wilcoxon rank sum test, chi-square test, or Fisher's exact probability test.

All statistical analyses were performed using Jump version 9.0 software. $P < 0.05$ was considered statistically significant.

Results

Pre- and postoperative blood work for splenectomy or PSE

Although we enrolled a total of 30 patients who underwent splenectomy/PSE, we excluded two patients who had

already undergone splenectomy in other hospitals because we could not obtain their data before splenectomy. Table 2 compares the pre- and postoperative blood work of the 28 patients who underwent splenectomy or PSE in our hospital. Twenty-six underwent splenectomy, and two had PSE. White blood cell and platelet counts increased significantly from 3,410 ± 1,268 to 5,126 ± 1,337/mm^3 ($P < 0.0001$) and from 6.0 ± 1.4 × 10^4 to 16.7 ± 5.1 × 10^4/mm^3 ($P < 0.0001$), respectively. Furthermore, total bilirubin (T-Bil) and PT significantly improved from 1.2 ± 0.5 mg/dl to 0.9 ± 0.5 mg/dl ($P = 0.0004$) and from 80.6 ± 13.2 to 84.2 ± 9.2 % ($P = 0.0153$), respectively.

The IFN dose

Figure 2 shows the IFN dose until 24 weeks based on platelet counts.

Patients given 80 % or more of the normal dose constituted 76.6 % (157/205 patients), 0 % (0/4 patients), 35.4 % (17/48 patients), 8.3 % (1/12 patients), and 60.0 % (18/30 patients) of groups A, B, C, D, and E, respectively. The administration rates in groups C and D were significantly lower compared to group A ($P < 0.0001$, $P < 0.0001$, respectively). Also, the administration rates in cirrhotic patients in group E were significantly improved compared to those in groups C and D who did not undergo either procedure ($P = 0.0337$, $P = 0.0024$, respectively).

Virologic response

Figure 3a shows the virologic response to PEG-IFN/RBV therapy.

Table 2 Clinical data of patients who underwent PSE or splenectomy

	Before PSE or splenectomy ($n = 28$)	After PSE or splenectomy ($n = 28$)	P value
White blood cells (/mm^3)	3,410 ± 1,268	5,126 ± 1,337	<0.0001
Hemoglobin (g/dl)	12.5 ± 2.2	12.2 ± 1.9	0.3736
Platelet count (×10^4/mm^3)	6.0 ± 1.4	16.7 ± 5.1	<0.0001
AST (IU/l)	58.0 ± 24.2	65.5 ± 31.6	0.0849
ALT (IU/l)	54.8 ± 24.9	54.9 ± 32.3	0.7155
Total bilirubin (mg/dl)	1.2 ± 0.5	0.9 ± 0.5	0.0004
Albumin (g/dl)	3.7 ± 0.5	3.7 ± 0.4	0.8030
PT percentage activity (%)	80.6 ± 13.2	84.2 ± 9.2	0.0153

AST Aspartate aminotransferase, *ALT* alanine aminotransferase

The SVR rates of patients with genotype 1b and a high viral load and patients with genotype 2a/2b were 36.0 % (82/228 patients) and 73.2 % (52/71 patients), respectively.

In chronic hepatitis groups A and B, the SVR rates of patients with genotype 1b and a high viral load and patients with genotype 2a/2b were 46.4 % (71/153 patients) and 80.4 % (45/56 patients), respectively.

In the cirrhosis groups C, D, and E, the SVR rates of patients with genotype 1b and a high viral load and patients with genotype 2a/2b were 14.7 % (11/75 patients) and 46.7 % (7/15 patients), respectively.

In both patients with genotype 1b and a high viral load and patients with genotype 2a/2b, the SVR rates of the cirrhosis group were significantly lower than those of the chronic hepatitis group ($P < 0.00001$, $P = 0.009$, respectively).

In patients with genotype 1b and a high viral load, the SVR rates in groups A, B, C, D, and E were 46.7 % (70/150 patients), 33.3 % (1/3 patients), 20.5 % (8/39 patients), 0 % (0/11 patients), and 12.0 % (3/25 patients), respectively.

In patients with genotype 2a/2b, the SVR rates in groups A, B, C, D, and E were 80.0 % (44/55 patients), 100 % (1/1 patient), 33.3 % (3/9 patients), 100 % (1/1 patient), and 60.0 % (3/5 patients), respectively.

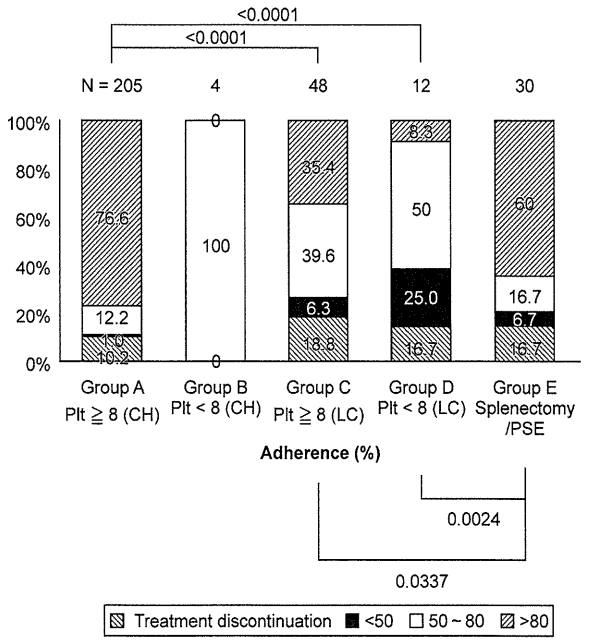

Fig. 2 The IFN dose until 24 weeks according to platelet count. The actual IFN dose rate until 24 weeks was evaluated as less than 50, 50–80, and 80 % of the normal dose. Group A, chronic hepatitis (plt ≥8); group B, chronic hepatitis (plt <8); group C, untreated cirrhosis group (plt ≥8); group D, untreated cirrhosis group (plt <8); group E, splenectomy/PSE

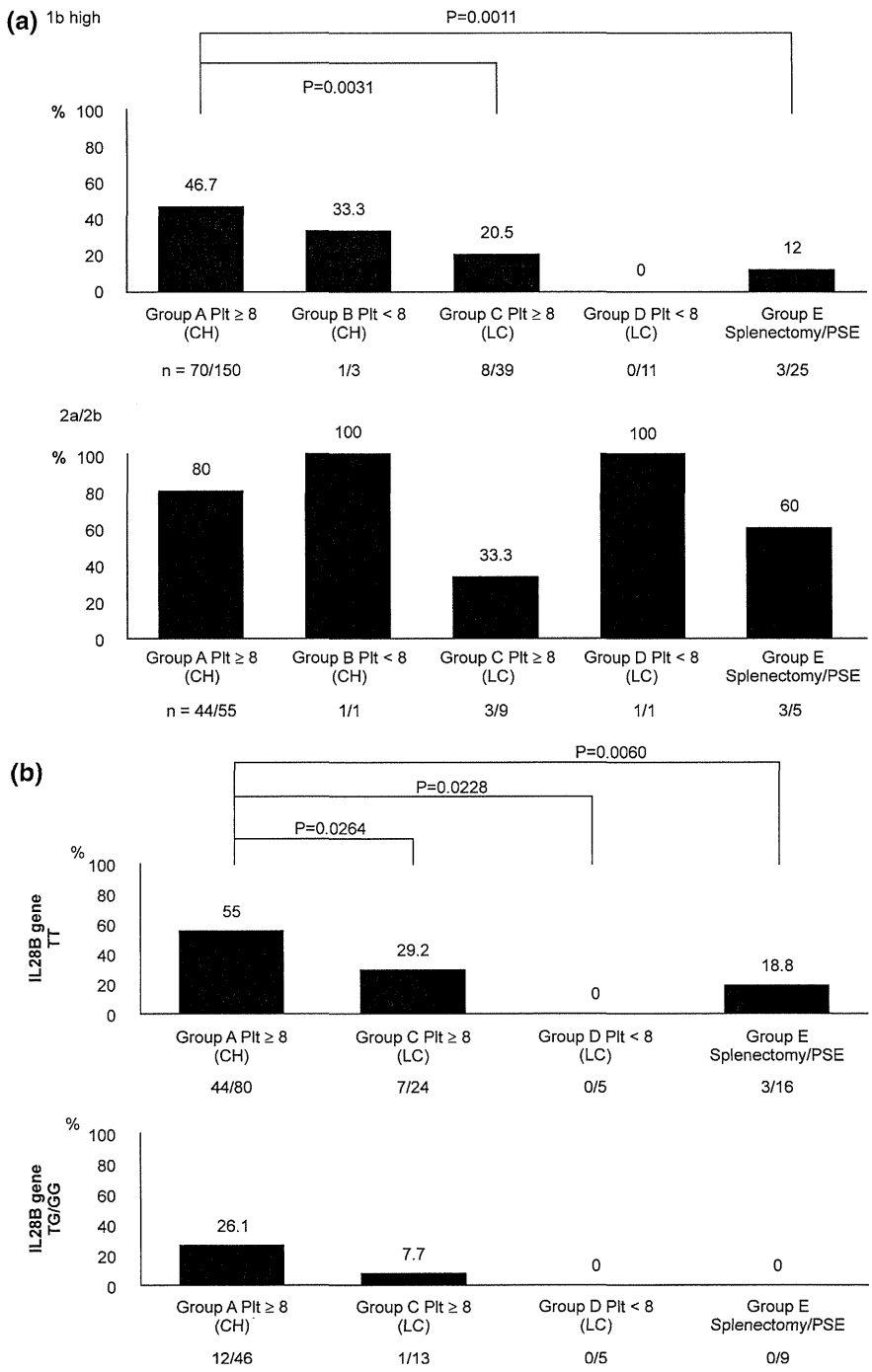

Fig. 3 **a** The sustained virological response (SVR) rate. **b** The SVR rate based on the IL28B genotype in patients with genotype 1b and high viral load. Twenty-five, two, and one patient from groups A, C, and D, respectively, were excluded because their IL28B genotype was not measured. Group B patients were excluded because only two patients underwent the examination